Syntectonic fluids redistribution and circulation coupled to quartz recrystallization in the ductile crust (Naxos Island, Cyclades, Greece)

Luc Siebenaller, Olivier Vanderhaeghe, Mark Jessell, Marie-Christine Boiron, Christian Hibsch

Syntectonic fluids redistribution and circulation coupled to quartz recrystallization in the ductile crust (Naxos Island, Cyclades, Greece)

Luc Siebenaller[a,b,*], Olivier Vanderhaeghe[a,b], Mark Jessell[b,c], Marie-Christine Boiron[a], Christian Hibsch[a]

[a] GeoRessources, Université de Lorraine, CNRS-CREGU, BP 70239, F-54506, Vandoeuvre-lès-Nancy, France
[b] Université de Toulouse, UPS GET, 14 avenue E. Belin, F-31400 Toulouse, France
[c] Centre for Exploration Targeting, The University of Western Australia, 35 Stirling Highway, Western Australia 6009, Australia

The presence of external fluids in metamorphic rocks has been shown to have a profound impact on rock rheology as high fluid pressure processes promote embrittlement and favor ductile deformation by recrystallization. Moreover, it has been proposed that brittle deformation guides fluid circulation and that intracrystalline deformation is responsible for fluid redistribution at the grain scale. Nevertheless, the amount of fluid present in the metamorphic ductile crust is debated and the nature of the interaction between fluids and recrystallization processes are not clearly identified. The aim of this study is to document the spatial distribution of fluid inclusions relative to microstructures in quartz grains and aggregates from veins sampled in amphibolite facies metamorphic rocks, exposed in the island of Naxos in the center of the Attic-Cycladic Metamorphic Complex in Greece. The veins, ranging from discordant structures with sharp contacts to totally transposed structures into the metamorphic foliation, display a large variety of microstructures and fluid evidences interpreted as recording exhumation processes through the ductile/brittle transition: (i) remnants of primary quartz grains contain abundant CO_2-H_2O fluid inclusions, decrepitated for the most part, distributed in clusters and in fluid inclusion trails, (ii) fluid inclusions with a similar composition are less abundant in recrystallized zones and in subgrains but are concentrated along grain boundaries indicating that grain boundary migration is responsible for redistribution of CO_2-H_2O fluids, (iii) subgrains of the last generation are almost devoid of fluid inclusions and are characterized by thick grain boundaries with abundant metamorphic fluids locally forming a continuous film. CO_2-H_2O fluid inclusions aligned in parallel, regularly spaced intragranular trails, locally rooted into grain boundaries, are interpreted as reflecting the spatial redistribution of these fluids in quartz slip planes owing to the increase of fluid pressure in grain boundaries. This proposition is corroborated by the parallelism between slip planes and fluid inclusion trails. Perpendicular sets of fluid inclusion trails formed at the junctions of subgrains suggest that redistribution of fluids along quartz slip planes contributes to the initiation of subgrain rotation recrystallization. Transgranular fluid inclusion planes oriented perpendicular to the regional mineral and stretching lineations of the host metamorphic rocks mark a transition from grain to rock scale brittle behavior associated with the infiltration of H_2O fluid, mixing to various degrees with the initial CO_2-H_2O fluid already present in the metamorphic rocks. These features indicate that, in the ductile-metamorphic crust, fluid redistribution is intimately linked to recrystallization mechanisms allowing fluids circulation under lithostatic pressure.

1. Introduction

The rheological behavior of the continental crust, which is subdivided into a brittle upper crust transitioning to a lower ductile crust, is accompanied by profound modifications on fluid distribution and circulations (Etheridge et al., 1983; Reynolds and Lister, 1987; Siebenaller et al., 2013). Investigations on fault zones have demonstrated that fluid circulation in the crust is intimately linked

* Corresponding author at: GeoRessources, Université de Lorraine, CNRS-CREGU, BP 70239, F-54506, Vandoeuvre-lès-Nancy, France.
E-mail address: luc_siebenaller@hotmail.com (L. Siebenaller).

to fracturing (Sibson et al., 1975; Etheridge et al., 1983; McCaig, 1988; Sibson, 2000; Ingebritsen and Manning, 2002). Indeed, the increase of fluid pressure causes a decrease in the strength of rocks and may induce rupture (Terzaghi, 1925). At higher temperature, although experimental work has shown that the presence of fluids promotes ductile creep (Griggs, 1967; Hobbs, 1968; Blacic, 1975; Tullis and Yund, 1989; Hirth and Tullis, 1992, 1994; Law, 2014), the causal relationship between metamorphic fluids and recrystallization has not been clearly identified. Moreover, the amount of fluids in the deep crust remains uncertain: some authors, invoking the small fluid/rock wetting angle at thermodynamic equilibrium and the efficiency of fluid escape through brittle fractures opened to the surface, propose that the amount of fluids in rocks under lithostatic pressure is limited to small disconnected pores (Yardley, 1986; Watson and Brenan, 1987; McCaig, 1988; Yardley and Valley, 1994). Others, in contrast, argue that the physical-chemical characteristics of fluids trapped in metamorphic rocks are consistent with establishment, at least locally and sporadically, of a grain-scale continuous fluid network (Jessell et al., 2003; Famin et al., 2004; Ingebritsen and Manning, 2010). Moreover, the production of internal fluids through metamorphic reactions or magma crystallization might augment the fluid/rock ratio and then destabilize the initial thermodynamic equilibrium between fluids and minerals, inducing crystallization of new metamorphic phases (Etheridge et al., 1983; Connolly, 1997; Oliot et al., 2010, 2014; Goncalves et al., 2012; Rossi and Rolland, 2014).

Studies on the distribution of fluid inclusions relative to microstructures suggest that intracrystalline deformation and microstructure development lead to the spatial redistribution of fluids at the mineral scale (Kerrich, 1976; Wilkins and Barkas, 1978; Bakker and Jansen, 1990; Drury and Urai, 1990; Boullier et al., 1991; Bons and Urai, 1992; Bakker and Jansen, 1994; Jessell et al., 2003; Schmatz and Urai, 2011). In particular, Wilkins and Barkas (1978) have identified that fluid inclusion trails tend to be localized along deformation lamellae and subgrain boundaries of quartz undergoing dislocation glide and recovery. Based on these observations, these authors propose that fluid at high-pressure in the cores of subgrains might diffuse into slip planes in the grain interior and assist dislocation propagation and climb. Similar results have been obtained by experimental deformation of quartz (Carter et al., 1964; Christie and Ardell, 1974; Fitz Gerald et al., 1991; Tarantola et al., 2010, 2012).

In order to complement these studies, in this paper, we present an analysis of fluid inclusions distribution relative to microstructures from quartz in veins enclosed in metamorphic rocks exhumed during the development of the Naxos Metamorphic Core Complex (MCC) in the Cyclades. This analysis allows us to investigate in natural examples (i) the relationship between the presence of fluids and quartz recrystallization and (ii) the impact of intracrystalline deformation on the spatial redistribution of fluids.

2. Geologic context: Naxos in the Attic-Cycladic Metamorphic Complex

Naxos Island, located in the center of the Aegean domain (Fig. 1a), is part of the Attic-Cycladic Metamorphic Complex (Dürr et al., 1978; Jacobshagen et al., 1978) and exposes rocks that have recorded burial and subsequent exhumation along the Africa-Eurasia convergent plate boundary (Dewey and Sengor, 1979; Dercourt et al., 1986; Jolivet et al., 2013; Scheffer et al., 2016). Naxos exposes the most complete structural section of the Cycladic Islands with a sequence of alternating schists and marbles juxtaposed along a low-angle detachment to an upper crustal unit comprising Miocene detrital sediments (Fig. 1b) (Jansen, 1973a,b; Buick, 1991; Gautier et al., 1993; Vanderhaeghe et al., 2007). Eocene relics of blueschist facies HP/LT metamorphism are preserved on the southern tip of the Island (Wijbrans and McDougall, 1986; Avigad and Garfunkel, 1991). They are overprinted by Miocene greenschist to amphibolite facies MT/MP metamorphism (Jansen and Schuiling, 1976; Buick and Holland, 1989; Duchêne et al., 2006). This metamorphism reaches partial melting as attested by the presence of migmatites coring a 10×20 km dome in the central part of the Island (Fig. 1b & c) (Keay et al., 2001; Martin et al., 2006, 2008; Vanderhaeghe, 2004; Kruckenberg et al., 2010, 2011). Metamorphic rocks are intruded by a syntectonic granodiorite pluton exposed along the western coast of the Island and dated at 12 Ma (Keay et al., 2001). Low-temperature thermochronology constrains exhumation of the crystalline rocks in the footwall of the detachment from 11 to 8 Ma (Brichau et al., 2006; Seward et al., 2009).

Naxos has been a target for the study of fluid circulation in metamorphic rocks. In particular, the presence of ubiquitous CO_2-H_2O fluid inclusions in the metamorphic rocks has animated a debate regarding the source of CO_2: some authors have invoked an origin of these fluids from a deep-seated mantle source (Rye et al., 1976; Schuiling and Kreulen, 1979; Kreulen, 1980, 1988) while others have favoured decarbonation of the nearby marbles together with dehydration of the schists and infiltration of H_2O-rich fluids issued from partial melting (Buick and Holland, 1991; Baker and Matthews, 1995). More recently, Siebenaller et al. (2013) have reconstructed the fluid history of rocks exhumed through the ductile/brittle transition with an initial trapping of CO_2-H_2O fluids associated with ductile deformation, followed by the infiltration of H_2O fluids associated with microscopic to macroscopic fracturing of the rock. Mineral and stretching lineations are homogeneously oriented N20° and kinematic criteria indicate a top-to-the-NNE sense of shear (Lister et al., 1984; Gautier et al., 1990; Urai et al., 1990; Buick, 1991; Vanderhaeghe, 2004).

3. Distribution of fluid inclusions relative to microstructures

In this study, building on the analysis of Siebenaller et al. (2013) that has documented the fluid record of rocks exhumed through the ductile/brittle transition, we focus on the distribution of fluid inclusions relative to microstructures. The studied samples consist of (i) discordant quartz veins cross-cutting transposed veins into the foliation of a leucogneiss layer affected by upper amphibolite facies metamorphism to the south of the Naxos migmatite dome, and (ii) a quartz vein transposed in a lower amphibolite facies biotite-schist to the north-west of the migmatite dome (Fig. 1b). These veins provide a microstructural and fluid record representative of deformation-retrogression from upper-amphibolite facies to greenschist facies coeval with exhumation through the ductile-brittle transition as evidenced by microstructures described in Siebenaller et al. (2013). The typology of the various quartz veins, their fluid inclusion and microstructural records as well as their formation and deformation P-T conditions are summarized in Table 1.

3.1. Quartz veins hosted by upper amphibolite facies leucogneiss

The leucogneiss displays three distinct sets of veins that are distinguished on the basis of their structural position. V-M2 veins with diffuse boundaries, sometimes structurally related to leucosomes and pegmatites, are totally transposed into the foliation and are interpreted to correspond to metamorphic veins affected by ductile deformation. V-BD N-S striking veins are discordant but partially transposed into the amphibolite-facies foliation and are interpreted to reflect successive episodes of brittle deformation of the leucogneiss during overall ductile deformation. V-B E-W strik-

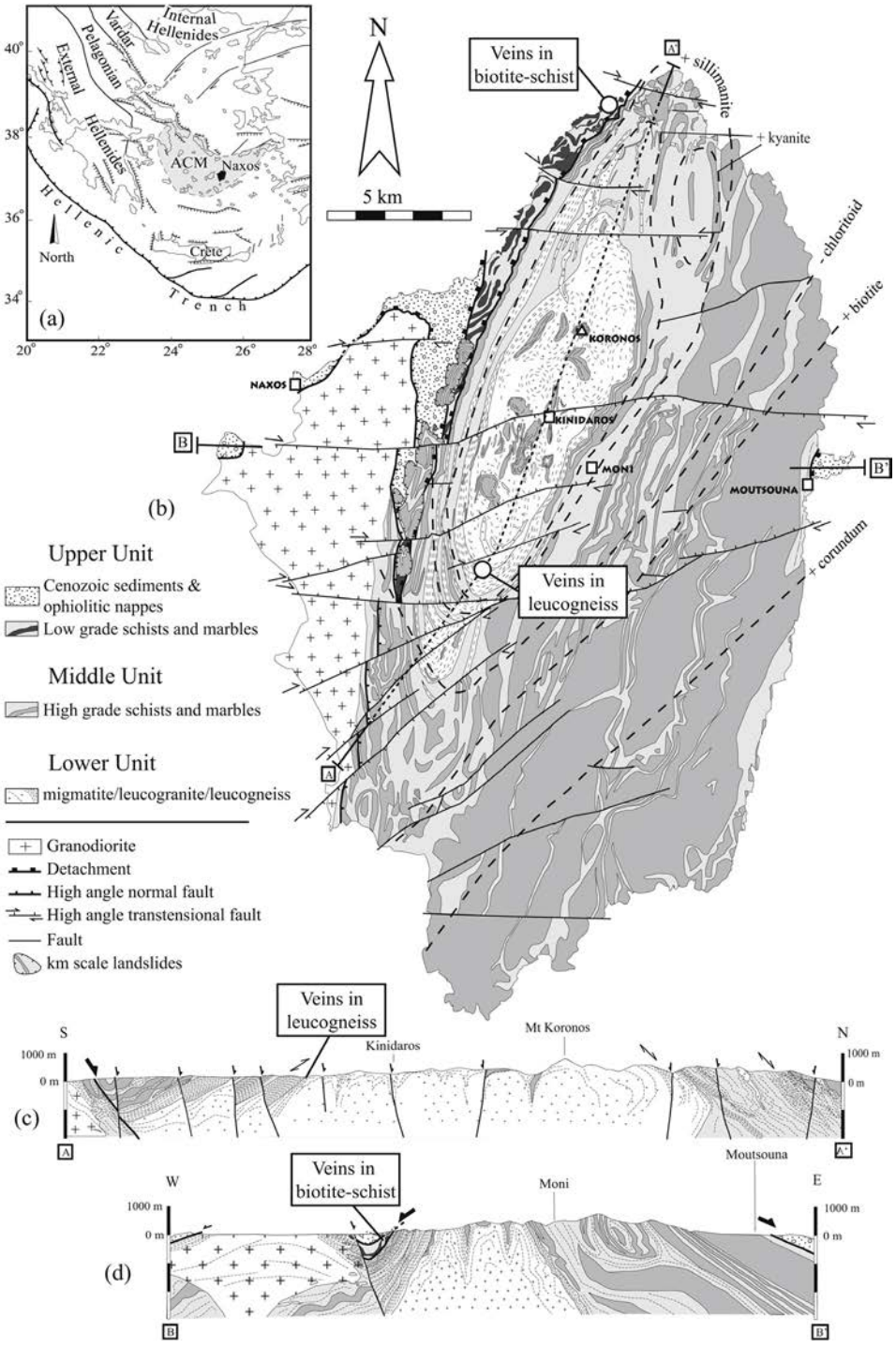

Fig. 1. (a) Geodynamic context of the Aegean region and localization of the Attic Cycladic Massif (ACM). (b) Geology of Naxos Island (modified after Jansen, 1973a; Vanderhaeghe, 2004; Siebenaller et al., 2013). (c) N–S cross-section (same legend as for Fig. 1b).

ing subvertical veins cross-cut the foliation with sharp contacts and are formed by brittle deformation. For field pictures, macrophotographs, veins structural relationships and more detailed field information, see Siebenaller et al. (2013).

3.2. Microstructures and fluid inclusions of transposed metamorphic veins V-M2

Totally transposed veins V-M2 display the most complete microstructural and fluid record (Figs. 2–4 and Fig. 3a & b from Siebenaller et al., 2013). These veins display a heterogeneous microstructure with remnants of primary centimeter-size grains, designated as Q_{rem}, showing a weak shape-preferred orientation and smaller subgrains, defined as Q_{rxt}, with variable sizes (Fig. 3a). Locally, older Q_{rem} quartz grains have preserved a core characterized by undulatory extinction, deformation bands, and chessboard texture but more generally they are subdivided into subgrains Q_{rxt} with a lower dislocation density indicative of dislocation glide associated with recovery by dislocation climb (Urai et al., 1986a; Hirth and Tullis, 1992) (Fig. 3a). The serrated Q_{rxt} grain boundaries are

Table 1
Unfolding of the structural evolution with respect to quartz vein formation, quartz grain microstructures, fluid inclusion typology and respective P–T trapping conditions (modified after Siebenaller et al., 2013).

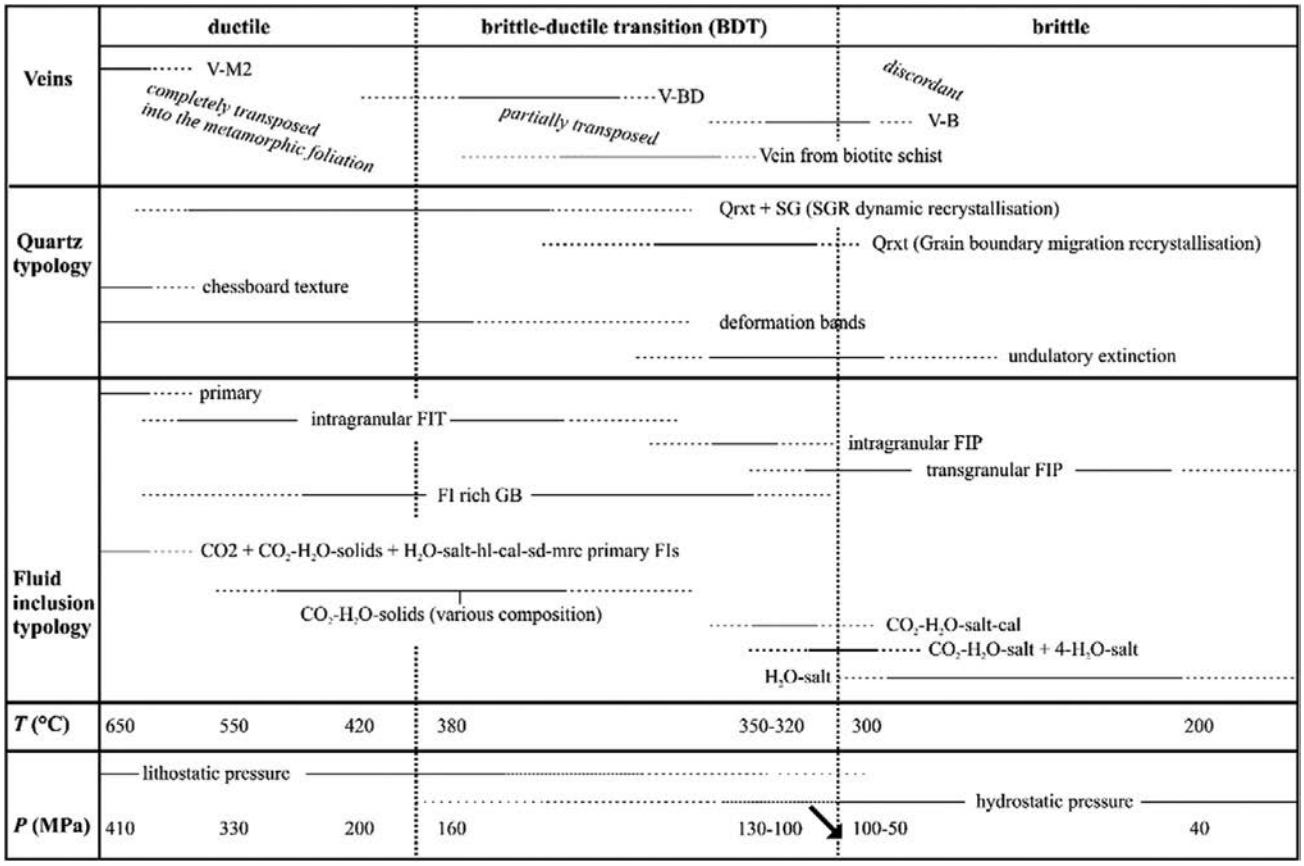

indicative of grain boundary migration (Fig. 3a). The presence of a mantle of small grains around older cores is interpreted to reflect recrystallization by subgrain rotation (SGR) (Guillopé and Poirier, 1979; Bons and Urai, 1992) (Fig. 3a & c).

The cores of older grains contain the most fluid inclusions in number and volume (Fig. 2 & b). These inclusions show a variety of compositions and microthermometric characteristics (see Siebenaller et al., 2013). They are dominated by mostly decrepitated CO_2, CO_2-H_2O, and H_2O highly saline fluids containing a variety of solids such as halite, siderite, calcite or marcasite and are organized as clusters or as curved intragranular fluid inclusion trails (FIT) with respect to completely recrystallized zones, preferentially localized along deformation bands. These fluid inclusion trails tend to have an N-S to NW-SE trend. Recrystallized zones (Q_{rxt}) and subgrains (SG) within older grains contain less fluid inclusions (Fig. 3a from Siebenaller et al., 2013). Subgrains mantling Q_{rem} grains are almost inclusion free and respective subgrain boundaries are rich in FIs (Fig. 3c, white arrows). Intragranular fluid inclusions in recrystallized zones have a CO_2-H_2O composition roughly similar to the one of fluid inclusions in Q_{rem} grains. Grain boundaries of Q_{rem} grains and boundaries of subgrains mantling older grains are rich in fluids and impurities, particularly at the intersection with intragranular fluid inclusion planes (FIP) (Fig. 3c). Locally, intragranular CO_2-H_2O FIT, trending at high-angle relative to each other, are rooted in grain boundaries (Figs. 3d & e). Recrystallized quartz grains are cross-cut by FIP with a steep dip of about 70° and a dominantly E-W trend (Figs. 2, 3 b & f), perpendicular to the regional scale stretching and mineral lineation. Some of these transgranular FIP contain CO_2-H_2O fluids while others contain solely H_2O. Intragranular CO_2-H_2O FIP display irregular shapes and variable liquid/vapor ratios (Fig. 4b). Many of the fluid inclusion trails contain decrepitated fluid inclusions that have collapsed in a plane perpendicular to the fluid inclusion trail with a limited lateral extension on both sides of the initial FIT (Fig. 4a). Such features have also been described in experimentally deformed fluid inclusions (Tarantola et al., 2010; their Fig. 7b & f). CO_2-H_2O transgranular FIP are geometrically connected to decrepitated annular primary fluid inclusions (Fig. 4c). This type of texture has been described by Pêcher (1981) from experimental work and by Boullier et al. (1991) from natural samples and are interpreted to be related to rapid decompression. H_2O transgranular FIP are also spatially connected to decrepitated larger fluid inclusions (Fig. 4d). Subhorizontal transgranular H_2O FIP exhibit striations (Fig. 4e & f). These striaes might correspond to the intersection between the plane of the inclusion and the transgranular FIP containing decrepitated fluid inclusions described above and illustrated in Fig. 4a.

3.3. Microstructures and fluid inclusions of partially transposed veins V-BD

Partially transposed veins V-BD display a microstructure characterized by millimeter-sized remnants of primary grains (Q_{rem}) that are smaller than the ones of V-M2 veins (Fig. 5). Q_{rem} grains have serrated grain boundaries, show undulatory extinction, deformation bands and are locally subdivided into micrometer-scale subgrains with a homogeneous extinction. Q_{rem} grains are partially recrystallized (Q_{rxt}) and surrounded by a mantle of subgrains (SG)(Fig. 5a & b).

In contrast to V-M2 totally transposed veins, V-BD partially transposed veins do not contain primary highly saline fluids. Relict

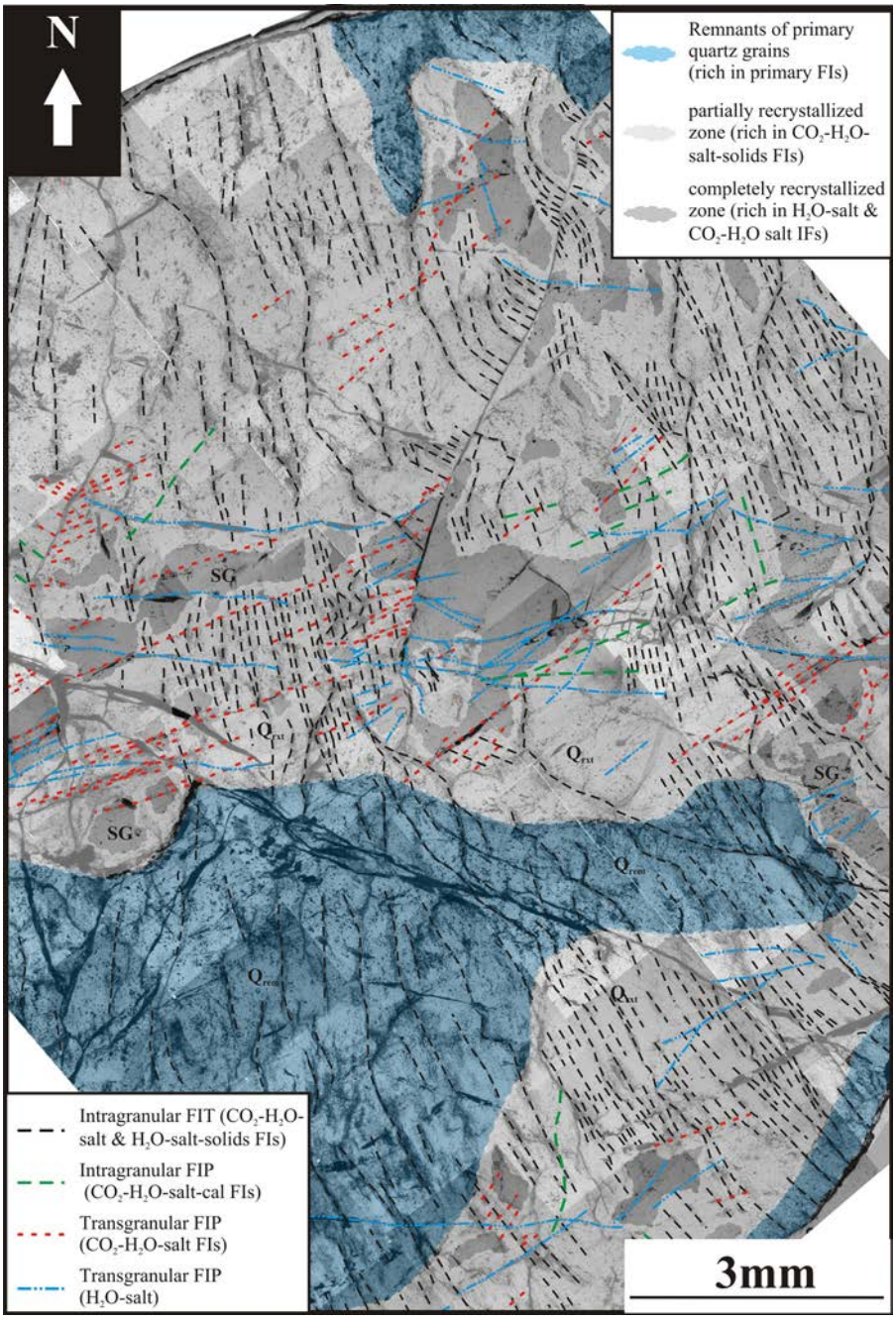

Fig. 2. Photomicrograph of thick section of V-M2 quartz vein (LS-04-115) and indication of fluid inclusion (FI) distribution in function of quartz microstructures. The regional stretching direction is N20. Remnants of primary quartz grains are bluish and surrounded by white dashed lines and are marked by a high density of primary FIs and N-S to NW-SE oriented fluid inclusion trails (FIT, black lines) of similar composition than primary FIs (c.f. Siebenaller et al., 2013; for a detailed description of the FI compositions). Light grey zones indicate parts of primary quartz grains that were affected by partial recrystallization. They contain remnants of primary FIs as well as N-S to NW-SE oriented FIT. The dark grey zones mostly located in the middle of the section are devoid of primary FIs and are marked by their poor FI content in general. They are organized along an E-W oriented zone crosscut by transgranular fluid inclusion planes (FIP, blue and red dashed lines). (For interpretation of the references to colour in this figure legend, the reader is referred to the web version of this article.)

primary grains contain abundant CO_2-H_2O fluid inclusions distributed as clusters and aligned in intragranular FIT (Fig. 5e). Subgrains mantling remnants of primary grains are spatially correlated with zones with the most fluid inclusions. However, the subgrains are almost inclusion free and fluid inclusions, impurities and oxides are found within or at the vicinity of recrystallized grain boundaries and subgrain boundaries (Fig. 5c & d). In some recrystallized grains, the former position of the Q_{rem} grain boundary is marked by a nearly continuous ring of fluid inclusions and impurities that have probably been left behind after grain boundary migration (Fig. 5e & f). Such textures are typical of grain boundary migration recrystallization (Drury and Urai, 1990).

3.4. Microstructures and fluid inclusions of discordant veins V-B with sharp cross-cutting contacts

Discordant veins V-B with sharp cross-cutting contacts show a simpler microstructure compared to V-M2 and V2-BD veins (Fig. 6). Remnants of centimeter sized primary quartz grains (Q_{rem}) with serrated grain boundaries are preferentially preserved in the cen-

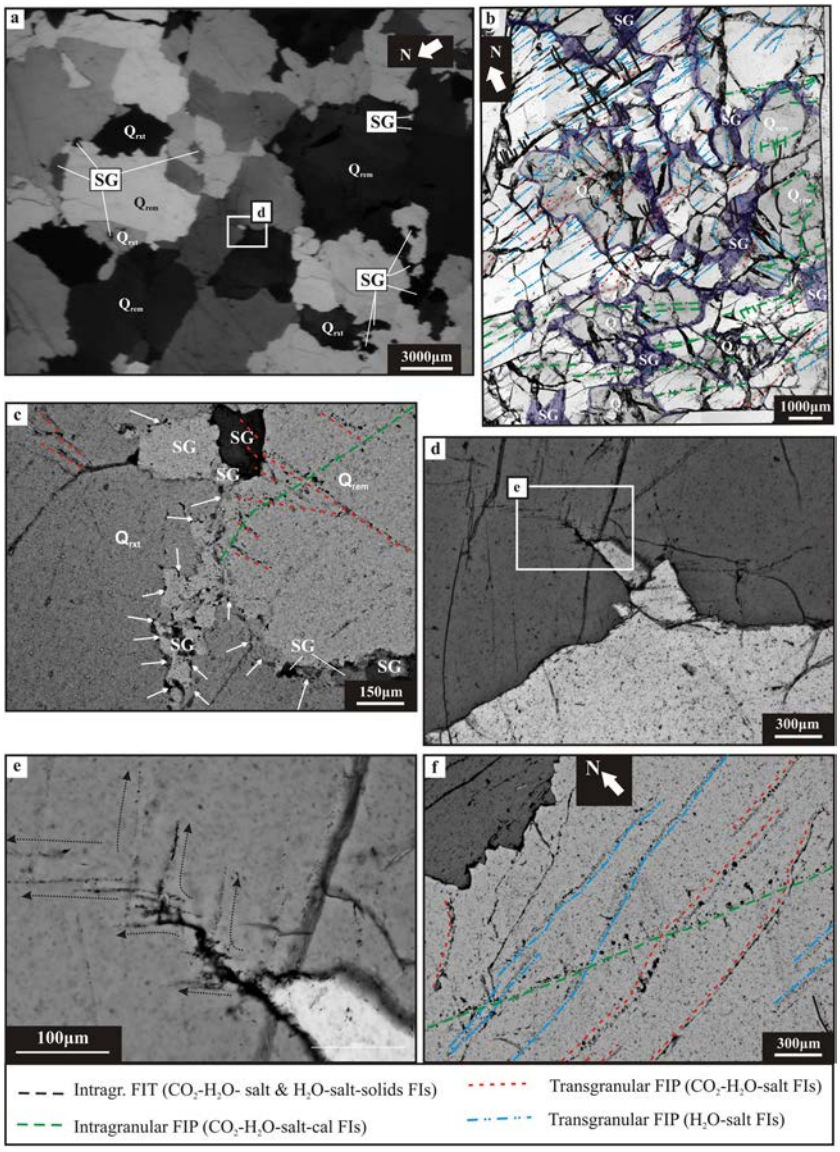

Fig. 3. Photomicrographs of V-M2 quartz vein (LS-06-17) showing the distribution of FIs in function of quartz microstructures. (a) Large view on quartz microstructures (cross-polarized light). Note the lobate and wavy grain boundaries and the presence of subgrains at the interface of larger grains. (b) Thick section with indication of FI distribution (c.f. Siebenaller et al., 2013; for a detailed description of the FI compositions). Q_{rem} are surrounded by a mantle of small-scale subgrains (SG) with inclusion rich grain boundaries (dark grey zones mantling Q_{rem}, of which a detail from a thin section is shown in c). Note that recrystallized zones are marked by a high amount of transgranular FIP (red and blue dashed lines). (c) Boundary between Q_{rxt} and Q_{rem} grains rich in fluid inclusion free subgrains (cross-polarized light). White arrows indicate Fi-rich lobate and wavy Q_{rxt}-Q_{rem} boundaries indicative grain boundary migration recrystallization. Recrystallized Q_{rxt} are devoid of intragranular FIP (green dashed line) and only crosscut by late transgranular FIP (red dashed lines). (d) Set of two small grains at the interface of two larger grains. (e) Zoom on apex of uppermost small grain from (d). Note a series of FIP perpendicular to each-other rooted into the nose of the grain boundary (dark part) that is marked by fluid inclusions that seem to propagate (indicated by black arrows) into the larger grain starting from the FI-rich grain boundary. (f) Close-up view on FIP organization in cross-polarized light. Transgranular FIP (CO_2-rich in red and H_2O-rich in blue) are closely spaced and all roughly E-W oriented. (For interpretation of the references to colour in this figure legend, the reader is referred to the web version of this article.)

ter of the veins and tend to be recrystallized along the walls (Fig. 7a). Wavy and lobate grain boundaries indicate grain boundary migration recrystallization (Fig. 6). Large Q_{rem} grains can also include subgrains and Q_{rxt} that have recrystallized by grain boundary migration (Fig. 7c, e & g). In these veins, all quartz grains display undulatory extinction but are devoid of deformation bands and do not present a shape preferred orientation (Siebenaller et al., 2013).

Veins V-B contain abundant fluid inclusions. Q_{rem} grains contain the most fluid inclusions as CO_2-H_2O distributed in clusters and in intragranular FIP (Fig. 7a & b). Fluid inclusions are less abundant in recrystallized grains Q_{rxt} and are distributed along intragranular FIT (Fig. 7a, b, d, e & g) as well as transgranular FIP (Fig. 7a & b). The intragranular FIT within recrystallized quartz Q_{rxt} are curved but have roughly the same orientation and fluid inclusions composition as intragranular FIP from Q_{rem} grains (Fig. 7e). They are in contrast to sharp fluid inclusion planes and contain decrepitated fluid inclusions with heterogeneous compositions. At the intersection between grain boundaries of recrystallized grains and intragranular FIP, the grain boundaries are particularly rich in fluid inclusions of similar composition (Fig. 7f). Based on these features, that are similar to the ones described in V-M2 veins (Fig. 3c), fluid inclusion trails are interpreted to represent former fluid inclusion planes that have been perturbed and redistributed by grain boundary migration recrystallization. Ghosts of former grain boundaries of Q_{rem} grains are underlined by rings of fluid inclusions and impurities (Fig. 7g & h). Some CO_2-H_2O fluid inclusion trails are rooted along

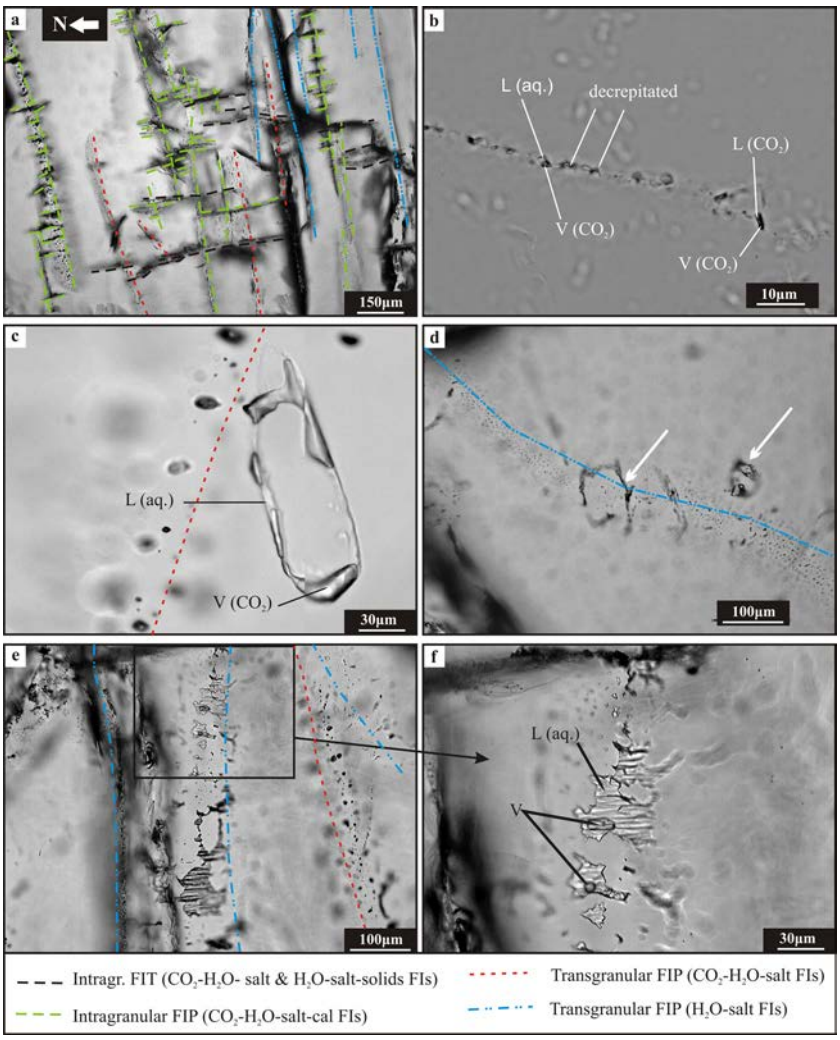

Fig. 4. Photomicrographs of thick sections of V-M2 vein (LS-06-17), showing FI textures. (a) Series of E-W oriented intragranular and transgranular FIP dipping at a high angle (zoom on Fig. 3b). Along intragranular FIP (green dashed lines) at places where large inclusions have decrepitated, small-scale perpendicular FIP are rooted and centered on the FIP inducing a perpendicular pattern of intragranular FIP. (b) FIs showing variable compositions and decrepitation features characteristic of FI from intragranular FIT (black dashed lines in (a)). (c) Association of large (>100 µm) annular decrepitated CO_2-rich FI and transgranular CO_2-rich FIP (red dashed line). L = Liquid, V = Vapor, aq. = water. (d) Association of large (>100 µm) annular decrepitated H_2O-rich FI (white arrows) and transgranular H_2O-rich FIP (blue dashed line). (e) and (f) flat and irregular FIs from E-W oriented late stage H_2O-rich sub horizontal FIP. Note the striation-like shaped internal surface of the FI. (For interpretation of the references to colour in this figure legend, the reader is referred to the web version of this article.)

grain boundaries and vanish at a few tens of microns away from them (Fig. 7i & j). These grain boundaries are rather thick and contain micrometer-size subgrains. Small subgrains within recrystallized older grains and cross-cutting larger subgrains are almost free of fluid inclusions but their grain boundaries are thick and characterized by a high density of fluid inclusions (Fig. 7b, e, g & h). Transgranular CO_2-H_2O and H_2O fluid inclusion planes cross-cut Q_{rem} as well as recrystallized Q_{rxt} grains (Fig. 7a, b & h). Transgranular CO_2-H_2O fluid inclusion planes cross-cut intragranular fluid inclusion trails with decrepitated inclusions (Fig. 7b & d).

3.5. Quartz veins in lower amphibolite facies biotite schist

At higher structural level, biotite-schists also contain numerous quartz veins that are totally to partially transposed in the metamorphic foliation (Fig. 8a). The studied sample was collected to the NW of the Naxos dome in lower amphibolite facies mylonitic rocks just beneath greenschist facies ultramylonite to cataclasite (Fig. 1). The microstructure is dominated by a shape preferred orientation of Q_{rem} grains (Fig. 8c). These older grains display an undulatory extinction, deformation bands, serrated and wavy grain boundaries were affected by recrystallization (Q_{rxt}). They are mantled by smaller subgrains exhibiting a shape-preferred orientation delineating the foliation (Fig. 8b, c & e). This microstructure is indicative of stress-driven subgrain rotation recrystallization (SGR). In these veins, SGR dominates but is associated with dislocation glide and recovery by grain boundary migration recrystallization. Together these microstructures reflect deformation at an intermediate temperature (~350 °C).

Q_{rem} grains are rich in CO_2-H_2O fluid inclusions distributed as clusters and fluid inclusion trails (Fig. 8d–i). Recrystallized grains and subgrains contain less abundant CO_2-H_2O fluid inclusions (Fig. 8b, d, f, g & i). Boundaries of subgrains are rich in disconnected fluid inclusions (Fig. 8d, g & h). Clusters of fluid inclusions and fluid inclusion trails in Q_{rem} grains show decrepitation textures and are connected to secondary fluid inclusion trails oriented perpendicular to the earlier ones (Fig. 8d & i) similar to those in Fig. 4a. Such features have been observed in experimental work by Tarantola et al., 2010 (c.f. Fig. 7b & f therein).

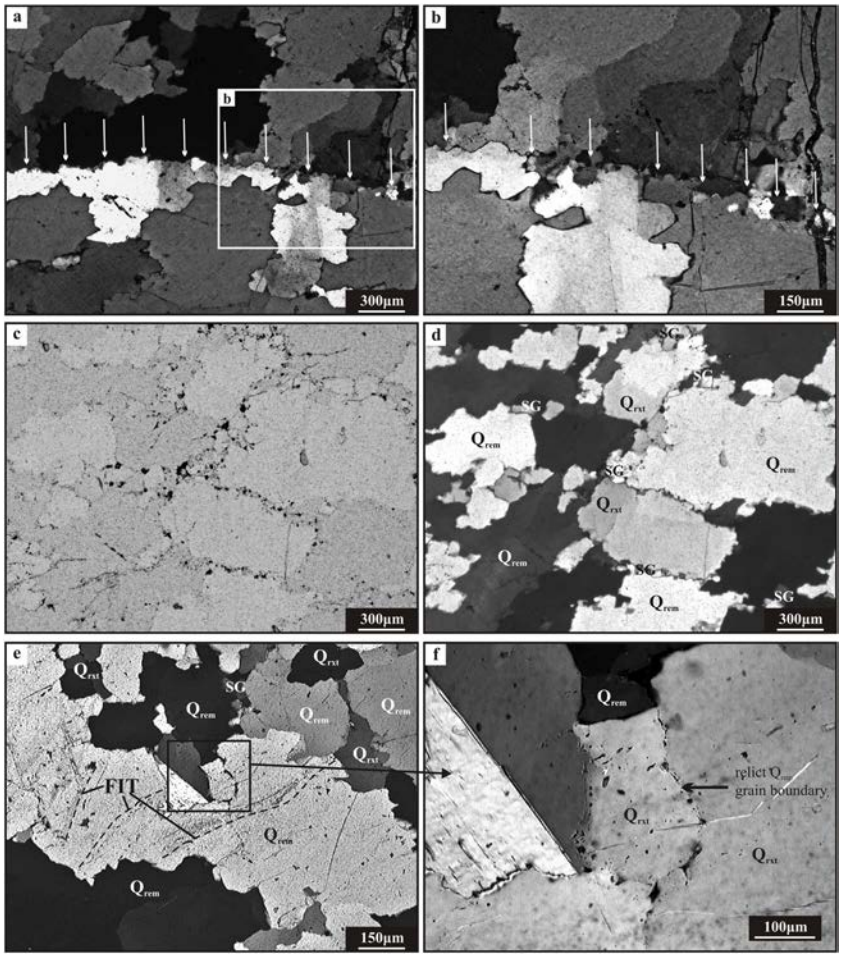

Fig. 5. Photomicrographs in cross-polarized light (except for (c), simple polarized light) of V-BD quartz veins. (a) and (b) micron-scale subgrains aligned within larger older grains (white arrows). (c) and (d) micron-scale subgrains (SG) mantling millimeter-size remnants of primary quartz grains (Q_{rem}). Note the high density of impurities (mostly oxides) and FIs (black dots) within subgrain boundaries. (e) and (f) Relict Q_{rem} grain boundary left over after recrystallization (Q_{rxt}). Note the near continuous ring of FIs and impurities (black dots) that mark the relict Q_{rem} grain boundary.

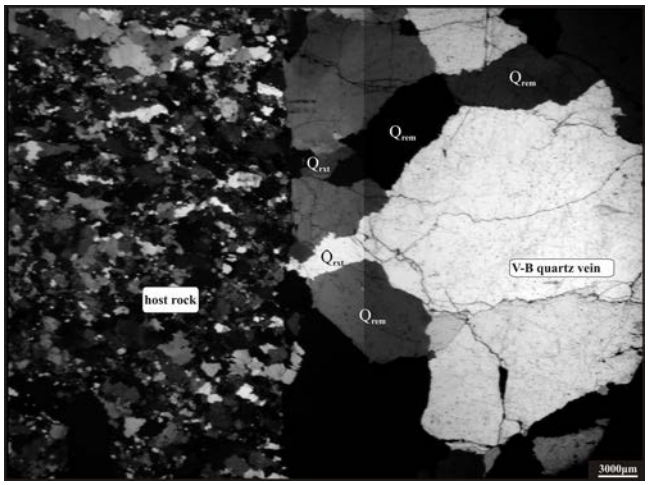

Fig. 6. Photomicrograph in cross-polarized light of V-B quartz vein (LS-06-33). Note the sharp cross-cutting contact with respect to the host rock and the large millimeter to centimeter-scale quartz grains showing lobate and wavy grain boundaries.

4. Discussion

The distribution of fluid inclusions relative to microstructure provides a basis to discuss the impact of quartz recrystallization on the redistribution of fluids and, in turn, on the impact of the presence of fluids on microstructure development. A summary of these features is given in Table 1.

4.1. Intracrystalline deformation and fluid redistribution

The fact that remnants of primary grains Q_{rem} are richer in fluid inclusions than recrystallized zones (grain boundary migration and subgrains formation) indicates that these processes induce a redistribution of fluids. This conclusion has already been reached via the analysis of naturally and experimentally deformed samples (Kerrich, 1976; Wilkins and Barkas, 1978; Drury and Urai, 1990; Bons and Urai, 1992; Jessell et al., 2003). The richness in fluid inclusions along serrated grain boundaries and along subgrain boundaries (e.g. Figs. 3 c, 5 c & 8 h) suggest that part of the fluid content of Q_{rem} grains is swept out by grain boundary migration and concentrated along the migrating grain boundaries (e.g. Urai et al., 1986a,b). Along subgrains within Q_{rem} grains, fluid inclusions are typically isolated but they locally form a continuous film along subgrains mantling recrystallized Q_{rem} grains (e.g. Fig. 7h).

However, the presence of intragranular fluid inclusions with a composition similar to the one of primary grains in zones affected by grain boundary migration (Figs. 3 c, 7 d–f & 8 d) and in subgrain boundaries (Figs. 3 c–e & 7 h) is consistent with a local redistribution of fluids associated with recrystallization. The analysis of experimentally-deformed natural and analogue materials

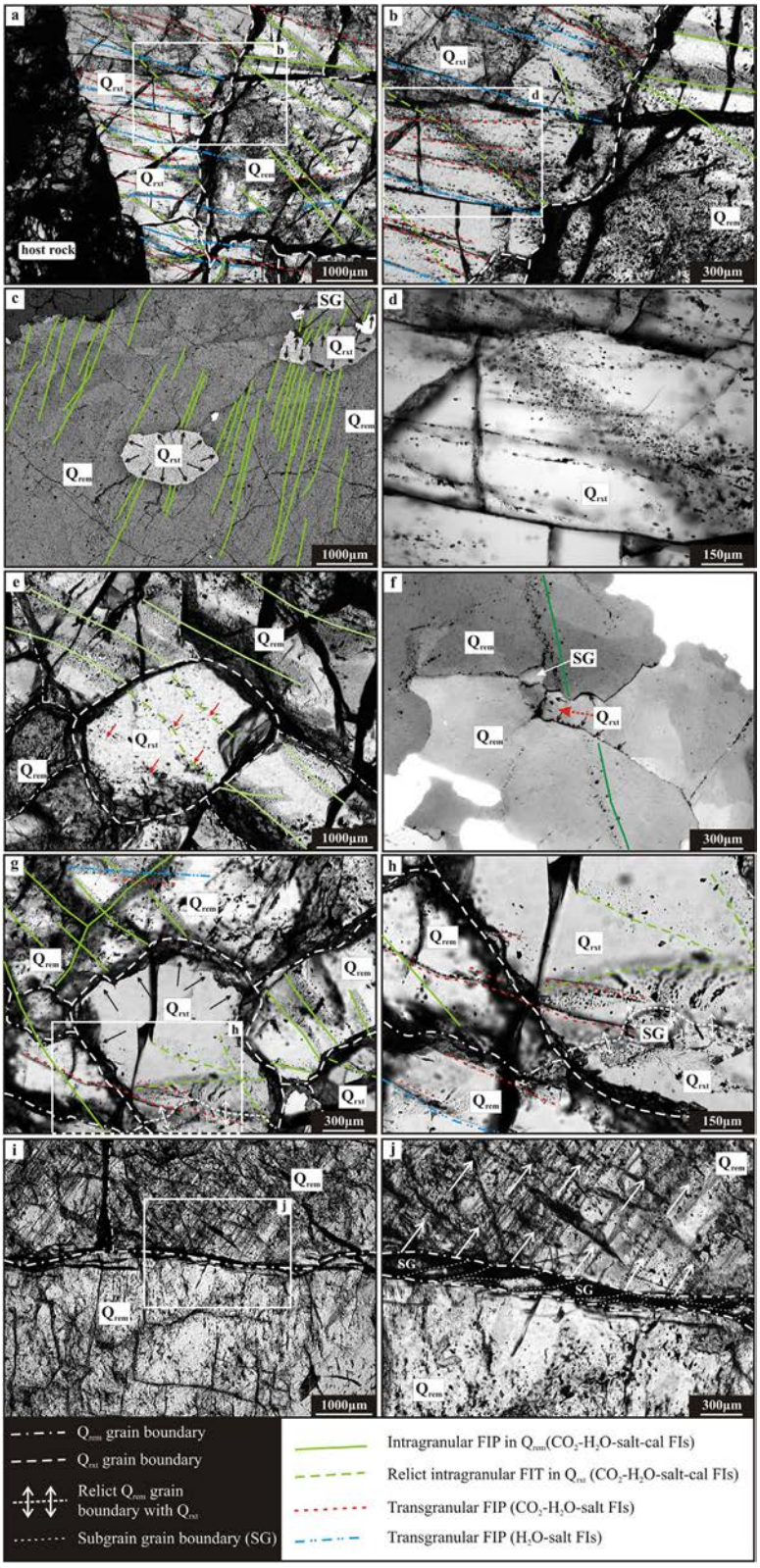

Fig. 7. Photomicrographs of thick (a, b, d, e, g–j) and thin (c, f) sections in cross-polarized light from V-B veins showing the distribution of FIs in function of microstructures. (a) Contact zone with the host rock. Note that the recrystallized quartz grains (Q_{rxt}) are rich in transgranular FIP whereas remnants of primary quartz grains (Q_{rem}) are rich in intragranular FIP and primary mostly decrepitated FIs (high density of dark dots). (b) zoom on (a) Intragranular FIT within Q_{rxt} mirror the orientation and composition of intragranular FIP within Q_{rem}. Note the very high density of primary decrepitated FIs clusters in Q_{rem} (right part). (c) high density of intragranular FIP (green lines) in large Q_{rem}. Q_{rxt} are devoid of intragranular. (d) zoom on (b) intragranular relict FIT do not show sharp planes as for FIP. (e) Zoom on similar texture as for (c) on thick section. Note that here remnants of FIs (intragranular FIT, indicated by red arrows) can be observed in Q_{rxt} following the same orientation as for intragranular FIP in Q_{rem}. Note also the thick fluid inclusion rich grain boundary of Q_{rxt} (black arrows). (f) intragranular FIP intersected by grain boundary of Q_{rxt}. Note the presence of FIs within or at the vicinity of the grain boundary (black arrows) at the locus where FI from FIP have been swept away by grain boundary migration recrystallization. (g) and (h) Recrystallized grain Q_{rxt} nearly devoid of FIs (black arrows), containing relict intragranular FIT similar to (f). Note the relict Q_{rem} grain boundary (bottom) marked by remnants of impurities and FIs. Transgranular FIP (red dashed lines) cross-cut Q_{rem} and Q_{rxt} grains. (i) et (j) Q_{rem} grain boundary marked by an alignment of subgrains. Note the high density of parallel intragranular FIP (white arrows) that are rooted into the Q_{rem} and subgrain boundaries. (For interpretation of the references to colour in this figure legend, the reader is referred to the web version of this article.)

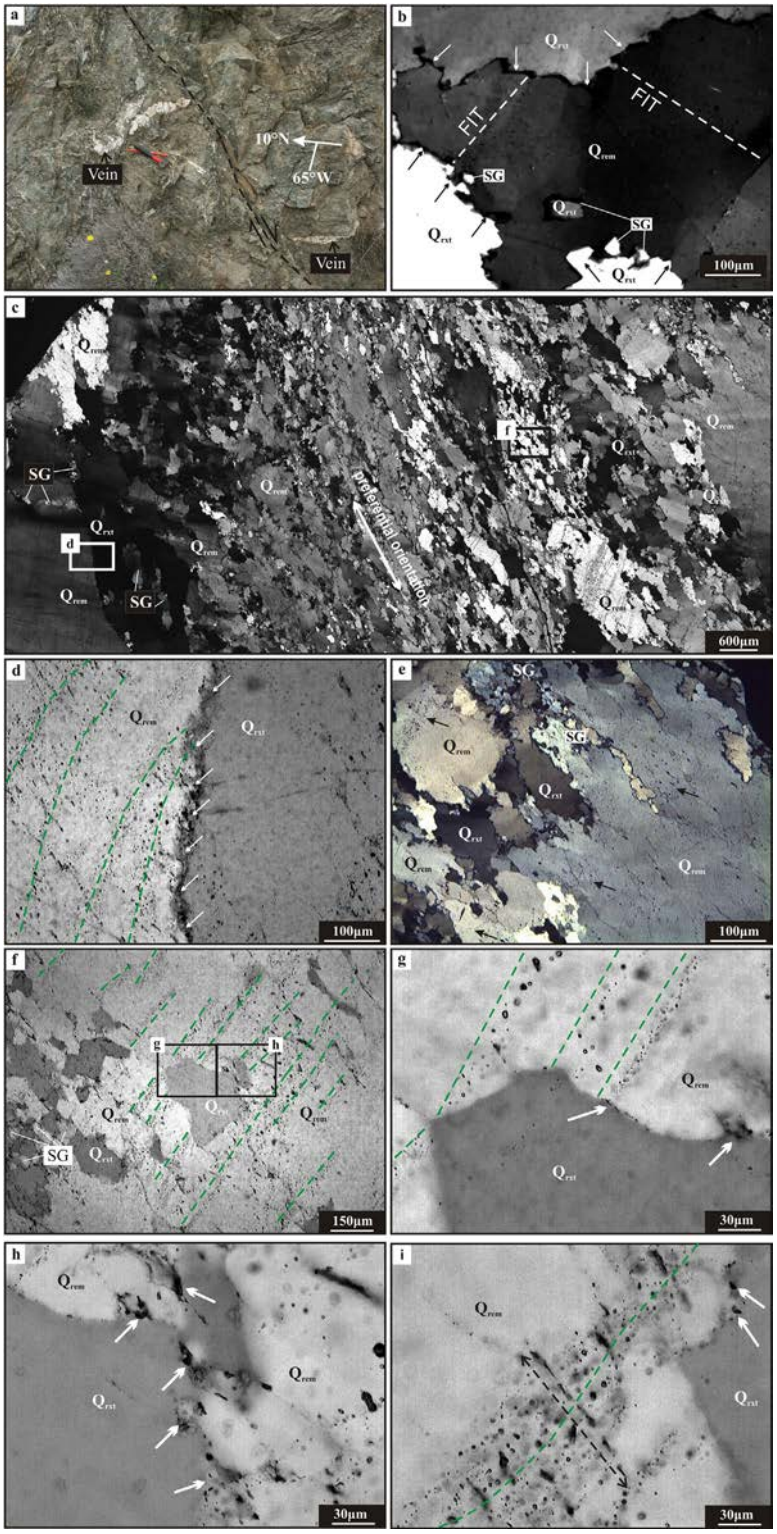

Fig. 8. Description of vein from lower amphibolite biotite-schist (LS-06-193). All figures except (a) correspond to photomicrographs in cross-polarized light. (a) Field photograph of vein partially transposed into the foliation of biotite-schist. (b) Typical lobate and wavy quartz grain boundaries, and evidences for undulose extinction and subgrain formation. (c) Large view on thin section showing quartz vein microstructures. The left and right edges of the figure are marked by large grains affected by undulatory extinction whereas the central part is characterized by a core and mantle structure where older grains (Q_{rem}) are partially recrystallized (Q_{rxt}) and mantled by subgrains indicating a preferential orientation. (d) zoom on grain boundary from large grains from left part in figure (c). White arrows indicate fluid inclusion rich $Q_{rxt} - Q_{rem}$ grain boundary. Note that Q_{rxt} is devoid of FIs at the contact whereas Q_{rem} is rich in intragranular CO_2-H_2O-salt-cal FIP (dashed green lines). (e) Remnants of primary grains (Q_{rem}) mantled by subgrains (SG). Subgrains and recrystallized grains (Q_{rxt}) show a preferential orientation and are devoid of fluid inclusions in contrast to Q_{rem} grains rich in fluid inclusion trails (black arrows). (f) Q_{rxt} are devoid of FIs at the contact whereas Q_{rem} are rich in intragranular CO_2-H_2O-salt-cal FIP (dashed green lines). (g) zoom on (f). White arrows indicate fluid inclusions along the $Q_{rxt} - Q_{rem}$ grain boundary. (h) FI-rich $Q_{rxt} - Q_{rem}$ grain boundaries (white arrows). Note the high FI content in Q_{rem} grains. (i) Zoom on intragranular FIT. Black dashed arrow in indicates fluid inclusion alignments centered on and perpendicular to the main fluid inclusion trail (green dashed line). (For interpretation of the references to colour in this figure legend, the reader is referred to the web version of this article.)

has shown that grain boundary migration and subgrain formation is more efficient at diminishing dislocation density than at redistributing fluids (Drury and Urai, 1990; Schmatz and Urai, 2010, 2011). This is consistent with the presence of CO_2-H_2O fluids within recrystallized grains Q_{rxt} (e.g. Fig. 7a, e & g). The interpretation of these features in terms of redistribution of CO_2-H_2O fluids associated with quartz recrystallization is further strengthened by the close spatial relationship between decrepitated primary CO2-H_2O inclusions with CO_2-H_2O inclusions aligned in trails. Decrepitation might be related to exhumation causing a decrease of the lithostatic pressure below the internal pressure of the fluid inclusions (Pêcher, 1981; Sterner and Bodnar, 1989; Boullier et al., 1991). Experimental work demonstrates that decompression-induced decrepitation leads to the production of ring-type inclusions (Boullier et al., 1991; Vityk and Bodnar, 1995; Tarantola et al., 2010). Decrepitation is also accompanied by a selective loss of the aqueous phase (Bakker and Jansen, 1990, 1994; Bakker and Diamond, 2006) which is consistent with the composition of primary fluid inclusions richer in CO_2 compared to intragranular fluid inclusion trails and the decrease in CO_2 for successive fluid inclusion trails. Exhumation of the Naxos' metamorphic rocks occurred during the Miocene as documented by their structural, petrologic, geochronologic and fluid record (Wijbrans and McDougall, 1986; Buick and Holland, 1989; Buick, 1991; Gautier et al., 1993; Duchêne et al., 2006; Brichau et al., 2006; Seward et al., 2009; Siebenaller et al., 2013)

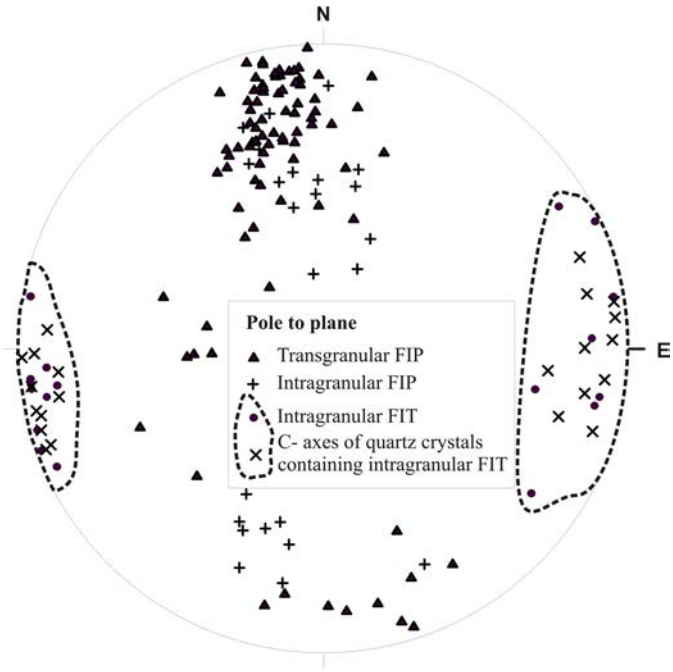

Fig. 9. Equal-area, lower-hemisphere projection of poles to plane for intragranular FIT and host quartz c-axes determined using a universal stage coupled to a microscope from V-M2 vein sample.

4.2. Fluid accumulation along grain boundaries, fluid pressure and infiltration of fluids in weak crystallographic planes

Accumulation of fluids along grain and subgrain boundaries leads to an increase in the fluid pressure if these fluids are not connected to the surface (Etheridge et al., 1983). This fluid pressure might overcome the strength of the rock and lead to embrittlement (Sibson et al., 1975; Etheridge et al., 1983). The distribution of fluid inclusions as intragranular fluid inclusion trails in recrystallized zones is reflecting a redistribution by fracturing at the grain scale of overpressured fluids accumulated along grain boundaries or within quartz grains after decrepitation of large inclusions and successive FI redistribution during grain boundary migration recrystallization. The regular spacing and parallelism of most intragranular fluid inclusion trails pleads for infiltration of fluids in a preferential weakness plane in the quartz grains that corresponds to the plane perpendicular to the quartz c-axis as indicated by their position perpendicular to intragranular FIP (Fig. 9). This interpretation is consistent with the results of experimental deformation of fluid inclusions enclosed in quartz grains (Tarantola et al., 2010, 2012), with recent work from the Snake range quartzite detachment (Carter et al., 2015) where similar features have been documented and with the localization of fluid inclusion trails along deformation bands (Wilkins and Barkas, 1978). According to this interpretation, the curved geometry of most inclusion trails suggests that they have been deformed after their formation. However, this interpretation is at odds with the dominant N-S trend of intragranular fluid inclusion trails which would require a strong crystallographic preferred orientation within the quartz veins. In contrast to intragranular fluid inclusion trails, the E-W orientation of transgranular FIP, perpendicular to the direction of extension (Fig. 9) and the fact that they cross-cut quartz grains irrespective of their crystallographic orientation (e.g. Figs. 2 & 3 b), indicates that they formed in response to fracturing beyond the grain scale.

4.3. Subgrain development and grain growth in zones of accumulated fluids

The spatial correlation between zones of fluid redistribution and subgrains within or around remnants of primary grains is consistent with the idea that recrystallization is favoured by the presence of fluids. The impact of fluids on dislocation creep has been shown by experimental work (Griggs, 1967; Hobbs, 1968; Hirth and Tullis 1992, 1994; Diamond et al., 2010). Although hydrolysis of Si-O bounds has been invoked (Griggs, 1967; Blacic, 1975), the nature of the link between the presence of fluids and recrystallization has not been clearly identified. Two situations are distinguished. First, on the inner side of growing older grain, the zone swept by grain boundary migration is characterized by the development of subgrains with fluid-rich grain boundaries (e.g. Figs. 3 c, 7 h, j & 8 g, h) suggesting a genetic link between these mechanisms. Second, on the outer side of growing older grains, the accumulation of fluids and impurities expelled from the migrating grain boundary is characterized by subgrains mantling remnants of primary grains with thick grain boundaries rich in fluid inclusions (e.g. Figs. 3 c, 7 h, j). In both cases, perpendicular sets of intragranular FIT rooted into subgrains (Figs. 4 a, 5 d–e & 7 i–j) where one of the fluid inclusion planes is perpendicular to the quartz c-axis and the other one parallel to the E-W oriented fractures (Fig. 9) suggest that the redistribution and infiltration of fluids, potentially into slip planes, facilitates the development of subgrains.

On the other hand, the spatial correlation between subgrains and transgranular fluid inclusion planes suggests also a genetic link between the infiltration of fluids in through-going fractures and recrystallization. The E-W trend of transgranular inclusion planes, perpendicular to the regional stretching and mineral lineation indicates that they formed during regional extension of the Aegean crust. These transgranular fluid inclusion planes are filled either by CO_2-H_2O fluid inclusions trapped at a temperature above 300 °C or by H_2O fluid inclusions trapped lower than 250 °C (Siebenaller et al., 2013). A temperature of more than about 350 °C is required for quartz recrystallization (Drury and Urai, 1990; Law, 2014), which is slightly more than the trapping temperature of fluid inclusions in transgranular fluid inclusion planes. The absence of intragranular fluid inclusions in subgrains and the presence of decrepitated fluid inclusions in older grains are consistent with pumping of the CO_2-H_2O fluids, already present in the metamorphic rock, into these

transgranular fluid inclusions. The lower trapping temperature of H_2O fluid inclusions suggests that they did not equilibrate thermally with the host minerals. Moreover, some H_2O might have mixed to various degrees with CO_2-H_2O fluid inclusions during redistribution into transgranular E-W trending planes.

The microstructural analysis provided in this paper indicates that recrystallization and fluid redistribution are intimately linked at the grain scale through a cycle involving (1) redistribution of fluids caused by recrystallization and grain boundary migration at the scale of quartz veins, (2) accumulation of fluids and buildup of fluid pressure along grain boundaries and within quartz grains as testified by the decrepitation of large fluid inclusions (Fig. 4c & d), (3) grain scale fracturing propagating from grain boundaries and leading to infiltration of fluids preferentially along crystallographic planes (Figs. 4 a, 5 d–e, 7 i–j & 9). This cycle of successive ductile deformation associated with intracrystalline deformation and brittle deformation caused by hydraulic fracturing is likely leading to transient permeability. Such a process might insure circulation of fluids under lithostatic pressure coeval with recrystallization and ductile deformation (Siebenaller et al., 2013). This gives some credit to the conceptual model of crustal-scale advective fluid transfer proposed by Etheridge et al. (1983). Transgranular fractures mark the transition from grain scale fracturing to at least vein scale brittle behavior. The H_2O composition and the isotopic signature of part of the fluids trapped in transgranular planes together with their microthermometric characteristics are consistent with the infiltration of a meteoric fluid and trapping under hydrostatic pressure suggesting that fractures were at least episodically connected to the surface at the time of exhumation of these rocks through the ductile/brittle transition (Siebenaller et al., 2013).

5. Conclusion

The relationships between microstructures and fluids inclusions, investigated on veins hosted by metamorphic rocks exposed in the Island of Naxos, indicate a link between recrystallization and fluid redistribution. Primary CO_2-H_2O fluid inclusions are preserved in the core of remnants of primary quartz grains. Recrystallization driven by dislocation glide, resulting in recovery and grain boundary migration, causes redistribution of fluids into fluid inclusion trails and toward grain boundaries. Grain boundaries of subgrains are locally characterized by a high density of fluid inclusions. The accumulation of fluids along grain boundaries are interpreted to be associated with an increase in fluid pressure triggering microfracturing, fluid infiltration along preferred quartz crystallographic planes and favouring subgrain rotation. These fluid inclusions are typically decrepitated or show variable CO_2-H_2O proportions suggesting fractionation during necking. Transgranular fracturing allows the infiltration of H_2O meteoric fluids which induces localized recrystallization, pumping of CO_2-H_2O fluids that are mixed with H_2O fluid and diluted.

Accordingly, the presence of fluids in high-grade metamorphic rocks impacts their microstructural development and intracrystalline deformation is responsible for grain scale redistribution of fluids that in turn control microfracturing along crystallographic planes and the formation of subgrains. This mechanism is likely to ensure fluid circulation under lithostatic pressure in the ductile-metamorphic crust.

Acknowledgments

We acknowledge A. Tarantola for insightful and stimulating discussions on quartz vein microstructures and fluid inclusion textures respectively. We thank C. Demeurie who prepared thin and thick sections. This work has been supported by the CNRS-INSU-3F (Fluid, Fault and Flow) program.

References

Avigad, D., Garfunkel, Z., 1991. Uplift and exhumation of high-pressure metamorphic terrains: the example of the Cycladic blueschist belt (Aegean Sea). Tectonophysics 188 (3–4), 357372.

Baker, J., Matthews, A., 1995. The stable isotopic evolution of a metamorphic complex Naxos, Greece. Contrib. Mineral. Petrol. 120, 391–403.

Bakker, R.J., Diamond, L., 2006. Estimation of volume fractions of liquid and vapor phases in fluid inclusions: and definition of inclusions shape. Am. Mineral. 91, 635–657.

Bakker, R.J., Jansen, J.B.H., 1990. Preferential water leakage from fluid inclusions by means of mobile dislocations. Nature 345 (6270), 58–60.

Bakker, R.J., Jansen, J.B.H., 1994. A mechanism for preferential H_2O leakage from fluid inclusions in quartz: based on TEM observations. Contrib. Mineral. Petrol. 116, 7–20.

Blacic, J.D., 1975. Plastic-deformation mechanisms in quartz: the effect of water. Tectonophysics 27, 271–294.

Bons, P.D., Urai, J.L., 1992. Syndeformational grain growth: micro-structures and kinetics. J. Struct. Geol. 14 (8–9), 1101–1109.

Boullier, A.M., France-Lanord, C., Dubessy, J., Adamy, J., Champenois, M., 1991. Linked fluid and tectonic evolution in the High Himalaya mountains (Nepal). Contrib. Mineral. Petrol. 107 (3), 358–372.

Brichau, S., Ring, U., Ketcham, R.A., Carter, A., Stockli, D., Brunel, M., 2006. Constraining the longterm evolution of the slip rate for a major extensional fault system in the central Aegean, Greece, using thermochronology. Earth Planet. Sci. Lett. 241 (1–2), 293–306.

Buick, I.S., Holland, T.J.B., 1989. The P-T-t path associated with crustal extension, naxos, cyclades, Greece. Geol. Soc. Spec. Publ. 43, 365–369.

Buick, I.S., Holland, T.J.B., 1991. The nature and distribution of fluids during amphibolite facies metamorphism, Naxos, (Greece). J. Metamorp. Geol. 9, 301–314.

Buick, I.S., 1991. Mylonite fabric development on naxos, Greece. J. Struct. Geol. 13, 643–655.

Carter, N.L., Christie, J.M., Griggs, D.T., 1964. Experimental deformation and recrystallization of quartz. J. Geol. 72, 687–733.

Carter, M.J., Siebenaller, L., Teyssier, C., 2015. Orientation, composition, and entrapment conditions of fluid inclusions in the footwall of the northern Snake Range detachment, Nevada. J. Struct. Geol. 81, 106–124.

Christie, J.M., Ardell, A.J., 1974. Substructures of deformation lamellae in quartz. Geology 2, 405–408.

Connolly, J.A.D., 1997. Devolatilization-generated fluid pressure and deformation-propagated fluid flow during prograde regional metamorphism. J. Geophys. Res. 102, 149–173.

Dürr, S., Altherr, R., Keller, J., Okrusch, M., Seidel, E., 1978. In: Cloos, H. (Ed.), The Median Aegean Crystal-Line Belt: Stratigraphy, Structure, Metamorphism, Magmatism, vol. 38. IUCG Sci. Rep., Alps, Apennines, Hellenides, pp. 455–477.

Dercourt, J., Zonenshain, L.P., Ricou, L.-E., Kazmin, V.G., Le Pichon, X., Knipper, A.L., Grandjacquet, C., Sbortshikov, I.M., Geyssant, J., Lepvrier, C., Pechersky, D.H., Boulin, J., Sibuet, J.-C., Savostin, L.A., Sorokhtin, O., Westphal, M., Bazhenov, M.L., Lauer, J.P., Biju-Duval, B., 1986. Geological evolution of the Tethys belt from Atlantic to the Pamir since the Lias. Tectonophysics 123, 241–315.

Dewey, J.F., Sengor, A.M.C., 1979. Aegean and surrounding regions: complex multiplate and continuous tectonics in a convergent zone. Geol. Soc. Am. Bull. 90, 84–92.

Diamond, L.W., Tarantola, A., Stünitz, H., 2010. Modification of fluid inclusions in quartz by deviatoric stress. II: experimentally induced changes in inclusion volume and composition. Contrib. Mineral. Petrol. 160, 845–864.

Drury, M.R., Urai, J.L., 1990. Deformation-related recrystallization processes. Tectonophysics 172 (3–4), 235–253.

Duchêne, S., Aissa, R., Vanderhaeghe, O., 2006. Pressure-temperature-time evolution of metamorphic rocks from naxos (Cyclades, Greece): constraints from thermobobarometry and Rb/Sr dating. Geodinamica Acta 19 (5), 301–321.

Etheridge, M.A., Wall, V.J., Vernon, R.H., 1983. The role of the fluid phase during regional metamorphism and deformation. J. Metamorph. Geol. 1, 205–226.

Famin, V., Philippot, P., Jolivet, L., Agard, P., 2004. Evolution of hydrothermal regime along a crustal shear zone Tinos Island, Greece. Tectonics 23, 1–23.

Fitz Gerald, J.D., Boland, J.N., McLaren, A.C., Ord, A., Hobbs, B.E., 1991. Microstructures in water-weakened single crystals of quartz. J. Geophys. Res. 96 (B2), 2139–2155.

Gautier, P., Ballèvre, M., Brun, J.-P., Jolivet, L., 1990. Cinématique de l'extension ductile à naxos et paros (Cyclades). Comptes Rendus de l'Académie des Sciences de Paris 310, 147–153.

Gautier, P., Brun, J.-P., Jolivet, L., 1993. Structure and kinematics of upper Cenozoic extensional detachment on Naxos and Paros (Cyclades Islands, Greece). Tectonics 12, 1180–1194.

Goncalves, P., Oliot, E., Marquer, D., Connolly, J.A.D., 2012. Role of chemical processes on shear zone formation: an example from the Grimsel metagranodiorite (Aar massif, Central Alps). J. Metamorph. Geol. 30 (7), 703–722.

Griggs, D.T., 1967. Hydrolitic weakening of quartz and other silicates. Geophys. J. 14, 19–31.

Guillopé, M., Poirier, J.P., 1979. Dynamic recrystallization during creep of single-crystalline halite: an experimental study. J. Geophys. Res. 84, 5557–5567.
Hirth, G., Tullis, J., 1992. Dislocation creep regimes in quartz aggregates. J. Struct. Geol. 14 (2), 145–159.
Hirth, G., Tullis, J., 1994. The brittle-plastic transition in experimentally deformed quartz aggregates. J. Geophys. Res. 99 (B6), 11731–11747.
Hobbs, B.E., 1968. Recrystallization of single crystals of quartz. Tectonophysics 6, 353–401.
Ingebritsen, S.E., Manning, C.E., 2002. Diffuse fluid flux through orogenic belts: implications for the world ocean. Proc. Nat. Acad. Sci. U. S. A. 99, 9113–9116.
Ingebritsen, S.E., Manning, C.E., 2010. Permeability of the continental crust: dynamic variations inferred from seismicity and metamorphism. Geofluids 10, 193–205.
Jacobshagen, V., Dürr, S., Kockel, F., Kopp, K.O., Kowalczyk, G., Berckhemer, H., 1978. Structure and Geodynamic Evolution of the Aegean Region. In: Cloos, H. (Ed.). IUGG Scientific Report, Stuttgart, Alps, Apennines, Hellenides, pp. 537–564.
Jansen, J.B.H., Schuiling, R.D., 1976. Metamorphism on Naxos: petrology and geothermal gradients. Am. J. Sci. 276, 1225–1253.
Jansen, J.B.H., 1973a. Geological Map of Naxos (1/50 000). Institute for Geology and Mineral Resources, Athens.
Jansen, J.B.H., 1973b. Geological Map of Greece, Island of Naxos. Institute for Geology and Mineral Resources, Athens, pp. 341.
Jessell, M.W., Kostenko, O., Jamtveit, V., 2003. The preservation potential of microstructures during static grain growth. J. Metamorph. Geol. 21 (5), 481–491.
Jolivet, L., Faccenna, C., Huet, B., Labrousse, L., Le Pourhiet, L., Lacombe, O., Lacomte, E., Burov, E., Denele, Y., Brun, J., Philippon, M., Paul, A., Salaun, B., Karabulut, H., Piromallo, C., Monie, P., Gueydan, F., Okay, A., Oberhänsli, R., Pourteau, A., Augier, R., Gadenne, L., Driussi, O., 2013. Aegean tectonics: strain localization, slab tearing and trench retreat. Tectonophysics 597–598, 1–33.
Keay, S., Lister, G., Buick, I., 2001. The timing of partial melting, Barrovian metamorphism and granite intrusion in the Naxos metamorphic core complex Cyclades, Aegean Sea, Greece. Tectonophysics 342, 275–312.
Kerrich, R., 1976. Some effects of tectonic recrystallization on fluid inclusions in vein quartz. Contrib. Mineral. Petrol. 59, 195–202.
Kreulen, R., 1980. CO2-rich fluids during regional metamorphism on Naxos (Greece): carbon isotopes and fluid inclusions. Am. J. Sci. 280, 745–771.
Kreulen, R., 1988. High integrated fluid/rock ratios during metamorphism at Naxos: evidence from carbon isotopes of calcite in schists and fluid inclusions. Contrib. Mineral. Petrol. 98 (1), 28–32.
Kruckenberg, S.C., Ferré, E.C., Teyssier, C., Vanderhaeghe, O., Whitney, D.L., Skord, J., Seaton, N., 2010. Viscoplastic flow in migmatites deduced from fabric anisotropy: an example from Naxos dome, Greece. J. Geophys. Res. 115 (9), B09401, http://dx.doi.org/10.1029/2009jb007012.
Kruckenberg, S.C., Vanderhaeghe, O., Ferré, E.C., Teyssier, C., Whitney, D.L., Chapman, A., 2011. Flow of partially molten crust and the internal dynamics of a migmatite dome, Naxos, Greece. Tectonics 30 (3), TC3001, http://dx.doi.org/10.1029/2010tc002751.
Law, R.D., 2014. Deformation thermometry based on quartz c-axis fabrics and recrystallization microstructures: a review. J. Struct. Geol. 66, 129–161.
Lister, G.S., Banga, G., Feenstra, A., 1984. Metamorphic core complexes of cordilleran type in the cyclades aegean sea, Greece. Geology 12, 221–225.
Martin, L., Duchêne, S., Deloule, E., Vanderhaeghe, O., 2006. The isotopic composition of zircon and garnet: a record of the metamorphic history of Naxos, Greece. Lithos 87 (3–4), 174–192.
Martin, L., Duchêne, S., Deloule, E., Vanderhaeghe, O., 2008. Mobility of trace elements and oxygen isotopes during metamorphism: consequences on geochemical tracing. Earth Planet. Sci. Lett. 267, 161–174.
McCaig, A.M., 1988. Deep fluid circulations in fault zones. Geology 16, 867–870.
Oliot, E., Goncalves, P., Marquer, D., 2010. Role of plagioclase and reaction softening in a metagranite shear zone at mid-crustal conditions (Gotthard Massif, Swiss Central Alps). J. Metamorph. Geol. 28, 849–871.
Oliot, E., Goncalves, P., Schulmann, K., Marquer, D., Lexa, O., 2014. Mid-crustal shear zone formation in granitic rocks: constraints from quantitative textural and crystallographic preferred orientations analyses. Tectonophysics 612–613, 63–80.
Pêcher, A., 1981. Experimental decrepitation and re-equilibration of fluid inclusions in synthetic quartz. Tectonophysics 78 (1–4), 567–583.
Reynolds, S.J., Lister, G.S., 1987. Structural aspects of fluid-rock interactions in detachment zones. Geology 15, 362–366.
Rossi, M., Rolland, Y., 2014. Stable isotope and Ar/Ar evidence of prolonged multiscale fluid flow during exhumation of orogenic crust: example from the Mont Blanc and Aar Massifs (NW Alps). Tectonics 33 (9), 1681–1709.
Rye, R.O., Schuiling, R.D., Rye, D.M., Jansen, J.B.H., 1976. Carbon, hydrogen, and oxygen isotope studies of the regional metamorphic complex at Naxos, Greece. Geochim. Cosmochim. Acta 40, 1031–1049.
Scheffer, C., Vanderhaeghe, O., Lanari, P., Tarantola, A., Ponthus, L., Photiades, A., France, L., 2016. Syn to post-orogenic exhumation of high-grade nappes: structure and thermobarometry of the western Attic-Cycladic metamorphic complex (Lavrion, Greece). J. Geodyn. 96, 174–193.
Schmatz, J., Urai, J.L., 2010. The interaction of fluid inclusions and migrating grain boundaries in a rock analogue: deformation and annealing of polycrystalline camphor–ethanol mixtures. J. Metamorph. Geol. 28, 1–18.
Schmatz, J., Urai, J.L., 2011. The interaction of migrating grain boundaries and fluid inclusions in naturally deformed quartz: a case study of a folded and partly recrystallized quartz vein from the Hunsrück Slate, Germany. J. Struct. Geol. 33, 468–480.
Schuiling, R.D., Kreulen, R., 1979. Are thermal domes heated by CO2-rich fluids from the mantle? Earth Planet. Sci. Lett. 43, 298–302.
Seward, D., Vanderhaeghe, O., Siebenaller, L., Thomson, S., Hibsch, C., Zingg, A., Holzner, P., Ring, U., Duchêne, S., 2009. Cenozoic tectonic evolution of Naxos Island through a multi-faceted approach of fission-track analysis. Geol. Soc. Spec. Publ. 321, 179–196, In: extending a continent: architecture, Rheology and Heat budget.
Sibson, R.H., Moore, J.M.M., Rankin, A.H., 1975. Seismic pumping – a hydrothermal fluid transport mechanism. J. Geol. Soc. London 131, 653–659.
Sibson, R.H., 2000. Fluid involvement in normal faulting. J. Geodyn. 29, 469–499.
Siebenaller, L., Boiron, M.-C., Vanderhaeghe, O., Hibsch, C., Jessell, M.W., André-Mayer, A.-S., Photiades, A., 2013. Fluid record of rock exhumation across the britlle-ductile transition during formation of a Metamorphic Core Complex (Naxos Island, Cyclades, Greece). J. Metamorph. Geol. 31, 313–338.
Sterner, S.M., Bodnar, R.J., 1989. Synthetic fluid inclusions-VII. Re-equilibration of fluid inclusions in quartz during laboratory-simulated metamorphic burial and uplift. J. Metamorph. Geol. 7, 243–260.
Tarantola, A., Diamond, L.W., Stünitz, H., 2010. Modification of fluid inclusion in quartz by deviatoric stress I: experimentally induced changes in inclusion shapes and microstructures. Contrib. Mineral. Petrol. 160, 825–843.
Tarantola, A., Diamond, L.W., Stünitz, H., Thust, A., Pec, M., 2012. Modification of fluid inclusions in quartz by deviatoric stress. III: Influence of principal stresses on inclusion density and orientation. Contrib. Mineral. Petrol. 164 (3), 537–550.
Terzaghi, C., 1925. Principles of soil mechanics. Eng. News-Record 95, 19–27.
Tullis, J., Yund, R.A., 1989. Hydrolytic weakening of quartz aggregates: the effects of water and pressure on recovery. Geophys. Res. Lett. 16 (11), 1343–1346.
Urai, J.L., Means, W.D., Lister, G.S., 1986a. Dynamic recrystallization of minerals. AGU Geophys. Monogr. 36, 161–199.
Urai, J.L., Spiers, C.J., Zwart, H.J., Lister, G.S., 1986b. Weakening of rock salt by water during. Nature 324 (6097), 554–557.
Urai, J.L., Shuiling, R.D., Jansen, J.B.H., 1990. Alpine deformation on naxos (Greece). In: Knipe, R.J., Rutter, E.H. (Eds.), Deformation Mechanisms, Rheology and Tectonics. Special Publication of the Geological Society, London, pp. 509–522.
Vanderhaeghe, O., Hibsch, C., Siebenaller, L., Martin, L., Duchêne, S., de St Blanquat, M., Kruckenberg, S., Fotiadis, A., 2007. Penrose conference -extending a continent -Naxos field guide. In: Lister, G.S., Forster, M., Ring, U. (Eds.), Inside the Aegean Metamorphic Core Complexes, vol. 27. Journal of the Virtual Explorer, pp. 1–30.
Vanderhaeghe, O., 2004. Structural development of the Naxos migmatite dome. In: Withney, D.L., Teyssier, C., Siddoway, C. (Eds.), Gneiss Domes in Orogeny. Geological Society of America Special Paper, Boulder, pp. 211–227.
Vityk, M.O., Bodnar, R.J., 1995. Textural evolution of synthetic fluid inclusions in quartz during reequilibration: with applications to tectonic reconstruction. Contrib. Mineral. Petrol. 121, 309–323.
Watson, E.B., Brenan, J.M., 1987. Fluids in the lithosphere. 1. Experimentally-determined wetting characteristics of CO_2-H_2O fluids and their implications for fluid transport, host rock physical properties and fluid inclusion formation. Earth Planet. Sci. Lett. 85, 497–515.
Wijbrans, J.R., McDougall, I., 1986. 40Ar/39Ar dating of white micas from an Alpine high-pressure metamorphic belt on Naxos (Greece): the resetting of the argon isotopic system. Contrib. Mineral. Petrol. 93, 187–194.
Wilkins, R.W.T., Barkas, J.P., 1978. Fluid inclusions: deformation and recrystallization in granite tectonites. Contrib. Mineral. Petrol. 65, 293–299.
Yardley, B.W.D., Valley, J.W., 1994. How wet is the earth's crust. Nature 371, 205–206.
Yardley, B.W.D., 1986. Fluid migration and veining in the Connemara Schists, Ireland. In: Walther, J.V., Wood, B.J. (Eds.), Fluid-Rock Reactions During Metamorphism, Advances in Physical Geochemistry, vol. 5. Springer-Verlag, New York, pp. 109–131.